Available online at www.sciencedirect.com
ScienceDirect
Electrochimica Acta 53 (2007) 1360–1364
ELECTROCHIMICA Acta
www.elsevier.com/locate/electacta

Investigation of bimetallic Pt–M/C as DMFC cathode catalysts

V. Baglio *, A. Stassi, A. Di Blasi, C. D'Urso, V. Antonucci, A.S. Aricò

CNR-ITAE Institute, via Salita S. Lucia sopra Contesse 5, 98126 Messina, Italy

Received 11 October 2006; received in revised form 17 April 2007; accepted 19 April 2007
Available online 5 May 2007

Abstract

A low temperature preparation procedure, based on a combination of colloidal and incipient wetness methods, was developed to modify the Pt catalyst with transition metals (Fe, Cu and Co). A moderate degree of alloying was obtained with Pt–Fe/C and Pt–Co/C cathode catalysts by using the new low temperature preparation route; whereas, a high degree of alloying was obtained for Pt–Cu/C by using the same procedure. Despite of the high metal concentration (60 wt%) on carbon, all catalysts showed small primary metal particle size and a low degree of agglomeration. These catalysts were investigated as cathodes in direct methanol fuel cells (DMFCs) operating at low temperatures (60 °C). It appeared that Pt–Fe/C catalysts were superior than Pt/C, Pt–Co/C and Pt–Cu/C catalysts both in terms of catalytic activity and tolerance to methanol. Adsorbed methanolic residues stripping analysis indicated a better methanol tolerance and an enhanced activity towards oxygen reduction in the case of the Pt–Fe system. An improvement of the DMFC single cell performance was also observed in the presence of Pt–Fe catalysts.

Keywords: Direct methanol fuel cells; Methanol tolerance; Pt–Co catalyst; Pt–Cu catalyst; Pt–Fe catalyst

1. Introduction

Stationary and automotive fuel cells (FC) devices are expected to play an important role for the sustainable energy generation in the next years [1–4]. Significant interest is also addressed to small portable fuel cells that possibly will find market application before large-size FC systems [5]. The potential market for portable fuel cell systems deals with remote and micro-distributed electrical energy generation including mobile phones, lap-top computers, energy supply for weather stations, medical devices, auxiliary power units (APU), etc. The main advantages of such systems rely on the high energy density of liquid fuels such as methanol and ethanol, long-life-time, easy recycle and low emission of pollutants in the environment [6–8]. Significant efforts are presently devoted to develop nanostructured catalysts for portable direct methanol and ethanol fuel cells. The target for DMFC/DEFC devices for portable application is to work at relatively low temperatures and atmospheric pressure with high efficiency and performance. The effective operation at this low temperature is particularly challenging and requires innovation in different aspects of materials and system development. In particular to address the poor reaction kinetics at the anode, high surface area catalysts composed of nanosised noble metal particles need to be developed and investigated for operation at low temperatures starting from sub-ambient to 60 °C [9–13]. Although, one of the main drawback of DMFC systems, i.e. the methanol cross-over through the membrane, is strongly depressed by the decrease of the operating temperature, this constraint affects the cathode performance even at low temperature by causing a mixed potential and poisoning of the cathode surface [14–18]. Accordingly, it is strongly necessary to develop methanol/ethanol tolerant cathode catalysts with suitable activity at low temperature. Also in this case, a proper catalytic activity for achieving portable fuel cells performance targets is assured by noble metal catalysts properly modified with transition metals capable of reducing the adsorption of alcohols on the cathode surface [19–26]. The activity presented in this paper deals with cathode catalysts synthesised by a low-temperature colloidal-incipient wetness route characterised by high concentration of metallic phase on carbon black and particle size smaller than 3 nm. Most of the previous studies were dealing with catalysts characterized by particle size larger than 3–4 nm and low concentration of active phase on carbon due to the need of high temperature treatment to form bimetallic alloys of transition metals with Pt [7,16,19]. Yet, in order to accelerate the oxygen reduction process a suitable number of

* Corresponding author. Tel.: +39 090 624237; fax: +39 090 624247.
E-mail address: baglio@itae.cnr.it (V. Baglio).

0013-4686/$ – see front matter © 2007 Elsevier Ltd. All rights reserved.
doi:10.1016/j.electacta.2007.04.099

surface sites is necessary. The developed preparation procedure has allowed to obtain carbon supported bimetallic nanoparticles with a particle size of about 2–2.5 nm and a suitable degree of alloying. However, high metal concentration catalysts are necessary to reduce the thickness of the catalytic layer, in particular when a high Pt loading is used to enhance the kinetics of oxygen reduction and methanol oxidation. Large thicknesses of the catalytic layer produce a decrease of electro-catalyst utilization and an increase in ohmic and mass transport polarization. The noble metal loading per cm^2 electrode area in fuel cells for portable application is usually larger than for stationary power generation or transportation, since the costs in this field are mainly determined by miniaturization.

The structure and morphology of the synthesised cathode catalysts has been investigated and these properties have been correlated with the electrochemical activity and tolerance to methanol poisoning.

2. Experimental

A 60 wt% Pt/Vulcan XC-72R was prepared starting from chloroplatinic acid by using the sulfite-complex route [27]. A $Na_6Pt(SO_3)_4$ precursor, obtained from chloroplatinic acid, was impregnated on Vulcan XC-72R carbon black and decomposed by adding H_2O_2 to form a Pt-oxide. Metallic Platinum supported on carbon (60% Pt/C) was obtained by reducing the PtOx/C in a H_2 stream. A 60 wt% Pt–Fe/Vulcan XC-72R, a 60 wt% Pt–Co/Vulcan XC-72R and a 60 wt% Pt–Cu/Vulcan XC-72R with a catalyst atomic composition Pt_3M_1 (which corresponds to about 5 wt% M content) were prepared starting from PtOx/Vulcan XC-72R by employing an incipient wetness method (using metal-nitrates as precursors) [28]. The bimetallic catalysts were reduced in a H_2 stream at room temperature. The obtained catalysts were characterized by recording the powders X-ray diffraction (XRD) pattern on a Philips X-pert 3710 X-ray diffractometer using Cu Kα radiation operating at 40 eV and 30 mA. The peak profile of the (2 2 0) reflection in the face centered cubic structure was obtained by using the Marquardt algorithm and used to calculate the crystallite size by using the Debye–Sherrer equation. X-ray Fluorescence analysis of the catalysts was carried out by a Bruker AXS S4 Explorer spectrometer operating at a power of 1 kW and equipped with a Rh X-ray source, a LiF 220 crystal analyzer and a 0.12° divergence collimator. The Pt/M atomic ratio was determined in all catalyst samples. Table 1 shows the physicochemical characteristics of the carbon supported Pt and Pt–M catalysts. TEM analysis was carried out by a Philips CM12 microscope.

Table 1
Physicochemical characteristics of Pt and Pt–M/C catalysts

Catalysts	Mean particle size (nm) (XRD)	Mean particle size (nm) (TEM)	Lattice parameter (A_0) (nm) (XRD)	Pt/M at. (XRF)
60% Pt/C	2.8	3.0	0.392	–
60% Pt–Fe/C	2.4	2.5	0.390	3.33
60% Pt–Cu/C	2.1	2.5	0.387	3.79
60% Pt–Co/C	2.3	2.5	0.389	3.50

To prepare the electrodes, a thin diffusion-layer comprising acetylene black and 20 wt% Teflon was firstly pasted onto a carbon cloth followed by the catalyst layer consisting of the catalyst with 15 wt% Nafion. An in-house 85% Pt–Ru alloy (1:1)/C catalyst was employed at the anode [12]; whereas, the 60% Pt/C and Pt–M/C catalysts were utilized for cathode fabrication. A Pt loading of 5 mg cm^{-2} was used for both anode and cathode. A Nafion 117 membrane was used as electrolyte. Membrane-electrode assemblies (MEAs) were formed by a hot-pressing procedure [29] and subsequently installed in a fuel cell test fixture of 5 cm^2 active area. This latter was connected to a test station including an HP6060B electronic load or to an EG&G electrochemical apparatus consisting of a PAR 273A Potentiostat/Galvanostat and a 20 A Current Booster. For single cell polarization experiments, aqueous methanol (1 M) was pre-heated at the same temperature of the cell and fed to the anode chamber of the DMFC through a peristaltic pump; dry air, pre-heated at the same temperature of the cell, was fed to the cathode. Atmospheric pressure in the anode and cathode compartments was used for all experiments. Reactant flow rates were 2 and 350 ml min^{-1} for methanol/water mixture and air stream, respectively. Single cell performances were investigated by steady-state galvanostatic polarization measurements. In half-cell polarization studies a three-electrode configuration was used. Hydrogen was fed to the cathode that was used as both counter and reference electrode. The anode polarization measurements were carried out by potentiodynamic sweeps at a scan rate of 5 mV s^{-1}. Data have not been corrected for the IR-drop. The cathode potential was deduced by adding the anode potential to the cell voltage.

In situ stripping voltammetry of adsorbed methanolic residues under DMFC configuration (feeding 1 M CH_3OH with a flow rate of 2 ml min^{-1} at the cathode and hydrogen on the other electrode) was carried out at 60 °C at carbon supported Pt and Pt–M catalysts/Nafion 117 membrane interfaces [12]. The first and second cycles were recorded at 50 mV s^{-1}, after adsorption from 1 M MeOH solution at 0.1 V for 30 min and subsequent washing by flowing deareated water through the electrode. Adsorption times longer than 30 min at 0.1 V did not appear to produce in our experiments any significant change in the stripping potentials and charge. In some cases small amounts of residual adsorbed CO was detected in the second scan. This residual amount was taken into account for a proper determination of the stripping charge.

3. Results and discussion

XRD patterns of Pt/C and Pt–M/C catalysts are reported in Fig. 1. They show the typical fcc crystallographic structure of Pt. A moderate degree of alloying was found for Pt–Fe catalysts; whereas, the degree of alloying was slightly larger for Pt–Co/C and significantly larger for Pt–Cu/C compared to Pt–Fe by using the same procedure. This is indicated by the decrease of the lattice parameter (Table 1). By using the Vergard's law, for the solid solution of these metals, the degree of alloying was calculated

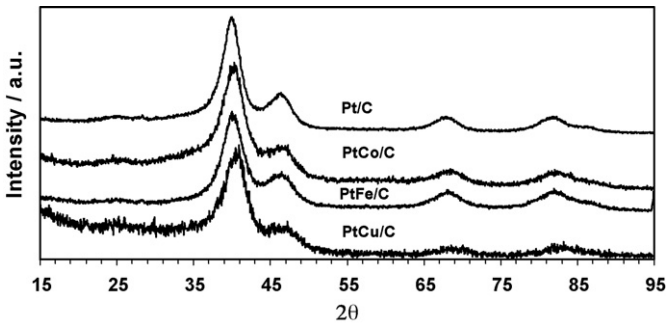

Fig. 1. XRD patterns of Pt and Pt–based bimetallic catalysts.

from the XRD determined lattice contraction. The calculated alloy compositions are 5% Fe–95% Pt, 8% Co–92% Pt, 21% Cu–79% Pt. Taking into account that chemisorption of oxygen on the electrocatalysts is the first step of the ORR, the geometrical influence of the Pt lattice constant is quite significant for the overall reaction [30]. A contraction of Pt lattice constant facilitates the dissociative O_2 adsorption; thus, the catalyst more strongly binds atomic oxygen [30]. As previously shown in the literature, Pt–Fe catalysts with small lattice constant contraction show a significant enhancement of the electrocatalytic activity for ORR [20]. The lattice constant contraction obtained by using this low temperature preparation route is small compared to Pt–Fe catalyst obtained by carbothermal reduction at high temperatures [21]. Although a large contraction in Pt–Fe lattice is favorable in terms of specific activity, recent studies

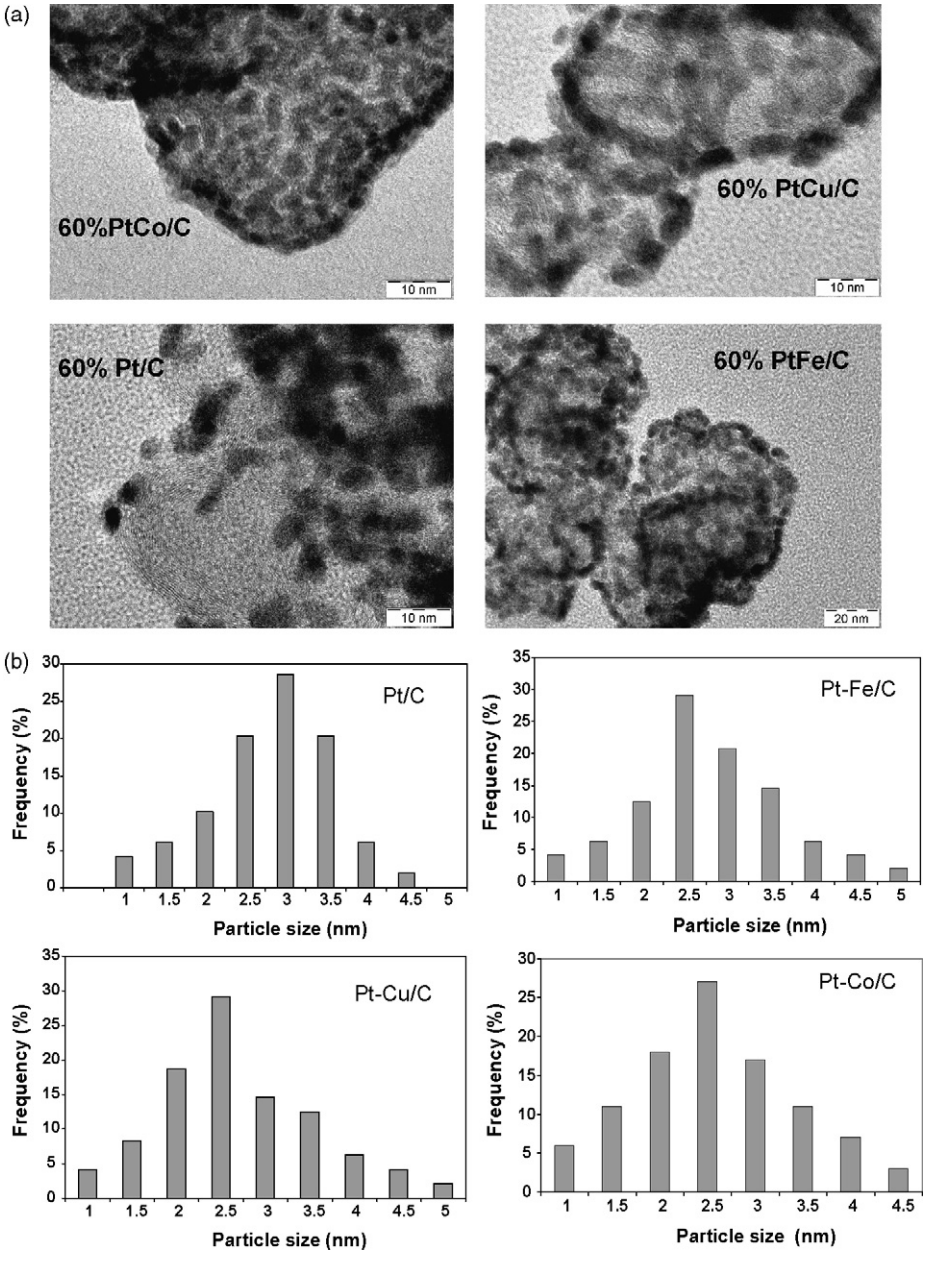

Fig. 2. TEM micrographs (a) and histograms (b) of Pt and Pt-based bimetallic catalysts.

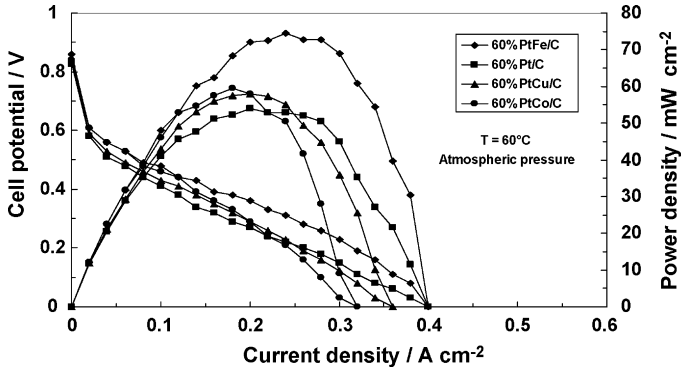

Fig. 3. Polarization and power density curves for the DMFCs equipped with the various cathode catalysts at 60 °C under atmospheric pressure.

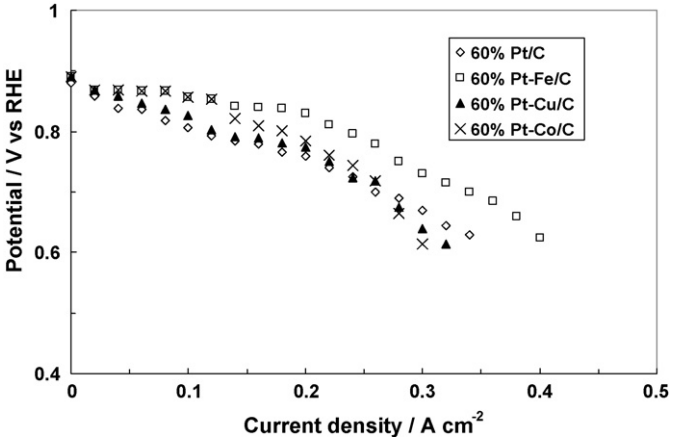

Fig. 4. Cathodic polarization curves for DMFCs based on the different cathode catalysts recorded at 60 °C under atmospheric pressure.

have shown that catalyst treatment at intermediate reduction temperatures, resulting in small Pt–Fe lattice contraction, are associated with a mass activity significantly higher than bare Pt catalysts [21].

TEM analysis of the catalysts shows a particle size distribution for the catalysts similar to that found by XRD measurements (Table 1) and a homogeneous distribution of fine metal particles on the support, despite of the high metal concentration on carbon (Fig. 2a and b).

For what concerns the polarization behaviour, the Pt–Fe/C (2.4 nm) performed better than the Pt/C, Pt–Cu/C and Pt–Co/C catalysts with similar particle size (2.1–2.8 nm) at 60 °C (Fig. 3). At low current densities (in the activation region) the performance of Pt–Fe/C and Pt–Co/C is almost the same and it is better than that obtained with Pt/C and Pt–Cu/C, indicating good properties of these catalysts towards the ORR in the presence of methanol. For Pt–Fe system, the open circuit voltage (OCV) is also higher than that recorded with the other catalysts; this indicates a higher methanol tolerance of this catalyst [31], since the same membrane was used in all experiments. The maximum power density recorded with Pt–Fe/C as cathode catalyst at 60 °C was about 75 mW cm^{-2}. At 0.5 V the current density was about 80 mA cm^{-2}. The cell equipped with the Pt–Cu/C catalyst at the cathode showed a lower performance in all the range of temperatures. A maximum power density of 58 mW cm^{-2} was recorded at 60 °C under atmospheric pressure. At 0.5 V the current density was about 60 mA cm^{-2} at 60 °C. The cell based on Pt–Co/C catalyst showed a maximum power density similar to that observed for the PtCu-based cell (about 60 mW cm^{-2}); whereas, at 0.5 V the current density was about 75 mA cm^{-2} at 60 °C, indicating a good catalytic behaviour for ORR and a suitable tolerance to methanol. At higher current densities the performance decreased due to a higher ohmic polarization. This could be due to Co leaching that poisons the membrane producing an increase of cell resistance. Lower performances (55 mW cm^{-2} maximum power density; current density at 0.5 V close to 55 mA cm^{-2}) were recorded with the cell equipped with the bare Pt/C cathode catalyst. The better performance of Pt–Fe catalyst for ORR is also confirmed by the cathode polarization curves (Fig. 4) that show almost the same trend of the cell polarizations, since the same anode was used in all the experiments. At low current densities, also the Pt–Co/C catalyst shows a proper combination of methanol tolerance and oxygen reduction activity properties. Yet, these suitable characteristics are lost at high current densities. Methanolic residues stripping analysis (Fig. 5) shows that this enhanced activity may derive from better methanol tolerance and higher intrinsic catalytic activity for oxygen reduction. The presence of a significant current density in the hydrogen desorption region ($E < 0.4$ V RHE) even after methanol adsorption, not observed for the other catalysts, indicates suitable methanol tolerance properties. The positive shift of the potential for PtO reduction is associated with a better intrinsic catalytic activity. The electrochemical active surface area as derived by the methanolic residues stripping analysis is larger for catalysts with smaller particle size (30.2 m^2/g for PtCu/C, 24.4 m^2/g for PtFe/C and 20.9 m^2/g for Pt/C). Yet, it appears that the small variation of electrochemically active surface area does not play the same role of the increase of methanol tolerance and intrinsic catalytic activity. In previous papers [12,13] it is reported that adsorbed methanolic residues stripping profiles are compared to the stripping of adsorbed CO. The peak potentials for the removal of adsorbed CO and methanolic residues are almost similar indicating that the adsorbed methanolic species are essentially CO-like species. Thus, it appears that the stripping behaviour is related to CO removal in both cases, but the steady-state coverage could

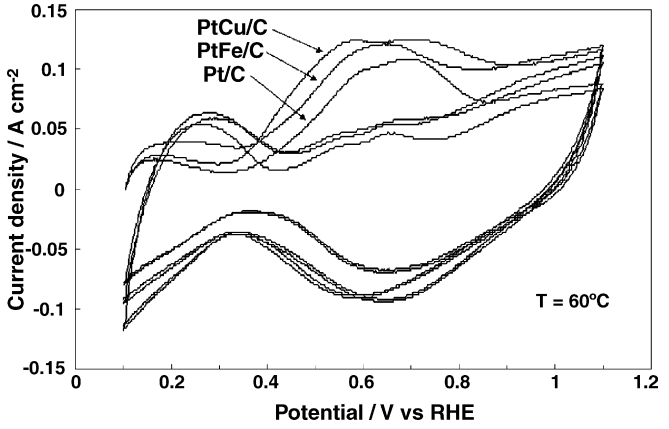

Fig. 5. Adsorbed methanolic residues stripping voltammetry at a scan rate of 50 mV s^{-1} for the different cathode catalysts at 60 °C.

be influenced by steric effects occurring in the first phase of methanol adsorption process [12]. Yet, the onset potential for the removal of the surface adsorbed methanolic residues is slightly lower than adsorbed CO indicating a possible surface rearrangement of the CO-like species after the methanol dehydrogenation step which reduces the adsorption strength between catalyst surface and adsorbate [13]. Due to the lower coverage of methanolic residues compared to adsorbed CO species derived from the adsorption of pure carbon monoxide, the electrochemical active surface area here reported are underestimated of about 20% [13].

The enhanced catalytic activity for Pt–Fe catalysts has been attributed to the presence of a Pt skin over the alloy together with an electronic effect induced by Fe on Pt, as previously reported by Watanabe and coworkers [19]. The formation of the Pt skin probably occurs because iron on the surface leaches out of the alloy during operation in acidic electrolytes, while Pt atoms are redeposited and rearranged on the surface. For what concerns the electronic effect, it was emphasized that the electronic structures of the Pt skin layers are altered by the underlying alloy substrates, which in turn facilitates the electron transfer to oxygen molecules [19]. On the other hand, Li et al. claimed that the improvement in the performance of Pt–Fe/C for ORR may be partly due to the higher peroxide decomposition activity of Pt in presence of dissolved Fe favoring the $4e^-$ transfer route [20]. In this respect, EDX measurements after operation showed a decrease in Fe content, revealing a partial ion dissolution during the work [31]. This may cause an increase in roughness and surface area, but the long-term stability of this system has to be confirmed by further experiments.

4. Conclusions

A preparation procedure was developed to modify the Pt catalysts with transition metals. A moderate degree of alloying was obtained with Pt–Fe/C cathode catalyst by using this low temperature preparation route. Whereas, the degree of alloying was slightly larger for Pt–Co/C and significantly larger for Pt–Cu/C compared to Pt–Fe by using the same procedure. High surface area carbon supported bimetallic Pt–Co, Pt–Cu and Pt–Fe catalysts were investigated for the oxygen electro-reduction process in low temperature direct methanol fuel cells (60 °C) and compared to Pt/C catalysts. Adsorbed methanolic residues stripping analysis showed a better methanol tolerance and an enhanced activity towards oxygen reduction in the case of the Pt–Fe system. An improvement of the DMFC single cell performance was also observed in the presence of Pt–Fe catalysts.

Acknowledgements

Financial support of the European Commission through the MOREPOWER Project No.: SES6-CT-2003-502652 is gratefully acknowledged. The authors express their appreciation to Prof. Ana Maria Castro Luna (INIFTA, La Plata, Argentina) for helpful discussions.

References

[1] A.S. Aricò, S. Srinivasan, V. Antonucci, Fuel Cells 2 (2001) 133.
[2] M. Neergat, D. Leveratto, U. Stimming, Fuel Cells 2 (2002) 25.
[3] S. Wasmus, A. Kuver, J. Electroanal. Chem. 461 (1999) 14.
[4] A.A. Kulikovsky, A. Kucernak, A.A. Kornyshev, Electrochim. Acta 50 (2005) 1323.
[5] R. Dillon, S. Srinivasan, A.S. Aricò, V. Antonucci, J. Power Sources 127 (2004) 112.
[6] X. Ren, M.S. Wilson, S. Gottesfeld, J. Electrochem. Soc. 143 (1996) L12.
[7] C. Lamy, S. Rousseau, E.M. Belgsir, C. Coutanceau, J.-M. Leger, Electrochim. Acta 49 (2004) 3901.
[8] W.J. Zhou, B. Zhou, W.Z. Li, Z.H. Zhou, S.Q. Song, G.Q. Sun, Q. Xin, S. Douvartzides, M. Goula, P. Tsiakaras, J. Power Sources 126 (2004) 16.
[9] T.C. Deivaraj, J.Y. Lee, J. Power Sources 142 (2005) 43.
[10] K.-T. Jeng, C.-C. Chien, N.-Y. Hsu, S.-C. Yen, S.-D. Chiou, S.-H. Lin, W.-M. Huang, J. Power Sources 160 (2006) 97.
[11] Z.-G. Shao, F. Zhu, W.-F. Lin, P.A. Christensen, H. Zhang, B. Yi, J. Electrochem. Soc. 153 (2006) A1575.
[12] A.S. Aricò, V. Baglio, A. Di Blasi, E. Modica, P.L. Antonucci, V. Antonucci, J. Electroanal. Chem. 557 (2003) 167.
[13] A.S. Aricò, V. Baglio, A. Di Blasi, E. Modica, G. Monforte, V. Antonucci, J. Electroanal. Chem. 576 (2005) 161.
[14] L. Jorissen, V. Gogel, J. Kerres, J. Garche, J. Power Sources 105 (2002) 267.
[15] J.R. Salgado, E. Antolini, E.R. Gonzalez, Appl. Catal. B: Environ. 57 (2005) 283.
[16] U.A. Paulus, A. Wokaun, G.G. Scherer, T.J. Schmidt, V. Stamenkovic, V. Radmilovic, N.M. Markovic, P.N. Ross, J. Phys. Chem. B 106 (2002) 4181.
[17] S. Mukerjee, S. Srinivasan, M.P. Soriaga, J.M. Mc Breen, J. Electrochem. Soc. 142 (1995) 1409.
[18] T.J. Schmidt, U.A. Paulus, H.A. Gasteiger, R.J. Behm, J. Electroanal. Chem. 508 (2001) 41.
[19] T. Toda, H. Igarashi, M. Uchida, M. Watanabe, J. Electrochem. Soc. 146 (1999) 3750.
[20] W. Li, W. Zhou, H. Li, Z. Zhou, B. Zhou, G. Sun, Q. Xin, Electrochim. Acta 49 (2004) 1045.
[21] M. Min, J. Cho, K. Cho, H. Kim, Electrochim. Acta 45 (2000) 4211.
[22] R.C. Koffi, C. Coutanceau, E. Garnier, J.-M. Leger, C. Lamy, Electrochim. Acta 50 (2005) 4117.
[23] H. Uchida, H. Ozuka, M. Watanabe, Electrochim. Acta 47 (2002) 3629.
[24] A.K. Shukla, R.K. Raman, Annu. Rev. Mater. Res. 33 (2004) 155.
[25] A.K. Shukla, R.K. Raman, N.A. Choudhury, K.R. Priolkar, P.R. Sarode, S. Emura, R. Kumashiro, J. Electroanal. Chem. 563 (2004) 181.
[26] H. Yang, C. Coutanceau, J.-M. Leger, N. Alonso-Vante, C. Lamy, J. Electroanal. Chem. 576 (2005) 305.
[27] H.G. Petrow, R.J. Allen, US Patent 3,992,331 (1976).
[28] V. Baglio, A.S. Aricò, A. Stassi, C. D'Urso, A. Di Blasi, A.M. Castro Luna, V. Antonucci, J. Power Sources 159 (2006) 900.
[29] A.S. Aricò, A.K. Shukla, K.M. el-Khatib, P. Cretì, V. Antonucci, J. Appl. Electrochem. 29 (1999) 671.
[30] Y. Xu, A. Ruban, M. Mavrikakis, J. Am. Chem. Soc. 126 (2004) 4717.
[31] A. Stassi, C. D'Urso, V. Baglio, A. Di Blasi, V. Antonucci, A.S. Aricò, A.M. Castro Luna, A. Bonesi, W.E. Triaca, J. Appl. Electrochem. 36 (2006) 1143.